

# Quantification of the QT Variability Related to HRV: Robustness Study Facing Automatic Delineation and Noise on the ECG

R Almeida<sup>1</sup>, E Pueyo<sup>2</sup>, JP Martínez<sup>2</sup>, AP Rocha<sup>1</sup>, P Laguna<sup>2</sup>

<sup>1</sup>Dep de Matemática Aplicada, Faculdade de Ciências Universidade do Porto, Portugal

<sup>2</sup>Comm Techn Group, Aragon Institute of Eng Research, University of Zaragoza, Spain

## Abstract

In this work we evaluated the robustness of an automatic system to study the relation between HRV and QTV. RR and QT series were measured by an automatic delineator and a low order linear model was used to explore their short term interactions and to quantify the QTV fraction related to HRV. Simulated series and artificial ECG signals were used to quantify the method performance, considering noise contamination of SNR from 30 to 10 dB. The errors found in the estimation of the QTV fraction related to HRV point out a non relevant performance decrease resulting from automatic delineation. The joint performance of delineation plus variability analysis is satisfactory for records presenting SNRs over 20 dB.

## 1. Introduction

The beat to beat ventricular repolarization variability (VRV) is known to be affected mainly by the heart rate variability (HRV), but also by other unrelated factors. These fractions are not yet completely characterized nor clearly quantified. Assessing this relation from QT and RR series, we explored the interactions by an improved version of a previously proposed dynamic linear approach [1].

Besides the smaller amplitude of QT variability (QTV) compared to HRV, one of this study main problems is the uncertainty in T wave end delineation. In clinical data, noise contamination increases delineation difficultness and can result in spurious QTV. We computed RR and QT intervals from automatic ECG delineation, avoiding intra/inter-observer variability. This previously developed wavelet transform based system has proven to be quite robust against noise and morphological variations [2].

The joint robustness of delineation and parametric approach was studied over controlled generated ECG signals, contemplating known relation of QT versus RR. Noise records were used to contaminate the ECG considering SNR levels from 30 to 10 dB in order to evaluate the accuracy lost in the estimation of QTV.

## 2. Methods

Our approach to assess VRV and HRV interaction (based on Porta et al [3]) was previously presented [1] and an enhanced version is under evaluation in this work. We consider  $RR(n)$  defined as the time interval from the previous to actual  $n$ th beat, and  $QT(n)$  as the QT interval related to the  $n$ th beat. All the series are zero-meaned.

### 2.1. Model formulation

We explored QTV and HRV interactions assuming an open loop linear model (Fig. 1) where  $A_{11}$ ,  $A_{12}$ ,  $A_{22}$  and  $D$  are  $z^{-1}$  polynomials with coefficients  $a_{11}(k)$ ,  $a_{12}(k)$ ,  $a_{22}(k)$  and  $d(k)$ .  $W_{RR}(n)$  and  $W_{QT}(n)$  are uncorrelated stationary zero-mean white noises (variances  $\lambda_{RR}^2$  and  $\lambda_{QT}^2$ ).  $RR(n)$  series was modelled as a  $p$  order AR ( $AR_p$ )

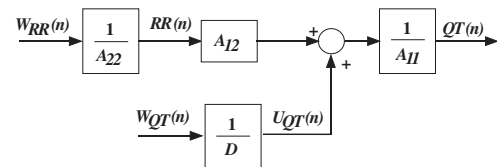


Figure 1. QTV versus HRV interactions model.

stationary random process and QT trend assumed to result from two uncorrelated sources, one driven by HR and other resulting of an exogenous input ( $ARARX_q$  model, [4])

$$RR(n) = - \sum_{k=1}^p a_{22}(k)RR(n-k) + W_{RR}(n) \quad (1)$$

$$QT(n) = \sum_{k=0}^q a_{12}(k)RR(n-k) + U_{QT}(n) - \sum_{k=1}^q a_{11}(k)QT(n-k)$$

$$U_{QT}(n) = - \sum_{k=1}^q d(k)U_{QT}(n-k) + W_{QT}(n). \quad (2)$$

For simplicity, the same order  $q$  was assumed for all ARARX polynomials, while a possible different order  $p$  is allowed for the AR model, which is a generalization from previous approaches where  $q = p$  was used [1, 3]. The order  $p$  represents the RR memory in its own past, while order  $q$  produces a cumulative memory effect between  $A_{11}$  and  $A_{12}$  or  $D$ , depending on the QT dependence considered. Note that  $q = p$  means double memory at  $QT(n)$  series than at  $RR(n)$  series.

The assumption of uncorrelated sources allows to compute the Power Spectral Density (PSD) of QT ( $S_{QT}(\Omega)$ ) as the sum of the partial spectra

$$S_{QT/W_{RR}}(\Omega) = T_R \lambda_{RR}^2 \left| \frac{A_{12}(z)}{A_{11}(z)A_{22}(z)} \right|_{z=e^{j\Omega T_R}}^2 \quad (3)$$

$$S_{QT/W_{QT}}(\Omega) = T_R \lambda_{QT}^2 \left| \frac{1}{A_{11}(z)D(z)} \right|_{z=e^{j\Omega T_R}}^2 \quad (4)$$

where  $\Omega = 2\pi f$  with  $f$  the frequency in Hz. As  $QT(n)$  and  $RR(n)$  series are unevenly sampled, the mean RR interval ( $T_R$ ) was used as the sampling period for estimating PSD functions, what has been shown acceptable for low frequencies far from the Nyquist frequency [5].

In each spectra  $S_E(\Omega)$ ,  $E \in \{QT/W_{QT}, QT/W_{RR}\}$ , the power was measured by PSD decomposition in components, each one corresponding to a pole  $p_k$ . A real  $p_k$  produces a real spectral component with power  $\gamma_k = \text{Res}[S_E(z)/z]$ , calculated at  $z = p_k$ ; complex conjugate poles  $p_k$  and  $p_k^*$  are associated to complex conjugate spectral components, which summed produce a real spectra with power  $\gamma_k + \gamma_k^* = 2\Re(\gamma_k)$ . The spectral power,  $P_E^B$ , in a frequency band  $B$ , is obtained by adding the contributions of the poles located in  $B$ . With  $c_k = 1$  for real and  $c_k = 2$  for complex conjugate poles,

$$P_E^B = \sum_{p_k \in B} c_k \Re(\gamma_k). \quad (5)$$

The algebraic decomposition of spectra does not guarantee admissible spectral components once negative estimates of power can occur, if the poles are close together [6]. Near the limit of a frequency band, this can originate a negative global contribution in a band, in which case the estimated model is considered inadequate and a different model order is selected. The relative contribution of QTV driven by RR in the frequency band  $B$  is given by

$$R_{QT/W_{RR}}^B = \frac{P_{QT/W_{RR}}^B}{P_{QT/W_{RR}}^B + P_{QT/W_{QT}}^B} \quad (6)$$

## 2.2. Model identification and order selection

The polynomial  $A_{11}$  was estimated from the series using least squares, while the ARARX model parameters

were iteratively obtained using a generalized least squares methodology [4]. A large enough SNR guarantees that the minima of the square residue are global [4] and convergence to residual white noise  $W_{QT}(n)$  is expected in a reasonable small number of iterations for adequate orders.

Orders  $p, q$  between 2 and 18 were considered to be adequate for modelling a given segment of data if the residual  $W_{RR}(n)$  and  $W_{QT}(n)$  can be considered uncorrelated white noises (5% significance bilateral test on the normalized autocorrelations, both in respect to the first 40 lags and all lags). Also were considered inadequate the model orders producing a negative global contribution in a frequency band, as described in the previous section. Optimal  $p$  and  $q$  were automatically selected from the obtained adequate orders as the ones that better satisfied the *Akaike Information Criteria* (AIC) [4].

## 2.3. Simulation and performance evaluation

The validation of the model was based on simulated  $RR(n)$  and  $QT(n)$  series of 350 consecutive beats with known QTV fraction correlated with RR ( $QT_{RR}(n)$ ).

Uncorrelated  $RR(n)$  series realizations were simulated, with 500 Hz sampling rate, using the Integral Pulse Frequency Modulation (IPFM) model [5], following  $AR_8$  modulating signals that match the spectra typically found at supine REST and head-up TILT situations (Fig. 2). Assuming that the linear model holds,  $QT(n)$  series were

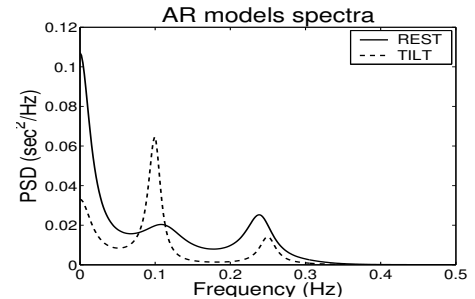


Figure 2. Spectra of  $AR_8$  models used in simulation.

simulated for each of the models (REST and TILT), using a priori chosen coefficients. The QT fraction driven by HRV ( $QT_{RR}(n)$ ) is obtained by filtering the simulated  $RR(n)$  whereas the non correlated fraction ( $QT_{QT}(n)$ ) is by filtering a simulated white noise with variance  $\lambda_{QT}^2$  ( $W_{QT}(n)$ ). The clean (“c”) test dataset was defined considering 50 uncorrelated realizations of each modulating signal and 3 cases of possible dependencies:

- $A_c$ : QT and RR fully correlated:  $QT(n) = QT_{RR}(n)$
- $B_c$ : QT and RR uncorrelated:  $QT(n) = QT_{QT}(n)$
- $C_c$ : Mix of  $A_c$  and  $B_c$ :  $QT(n) = QT_{RR}(n) + QT_{QT}(n)$ .

To evaluate the methodology in a more realistic context we constructed artificial ECG signals corresponding to each of the previous dataset elements. A clean and well defined template beat chosen from real files was baseline corrected and the interval from QRS end to T end was scaled to reflect the variability characteristics of the described  $QT(n)$  series. The ECG was obtained by concatenation of the modified beats following the  $RR(n)$  beat intervals. The ECG fiducial marks were obtained using the automatic delineation system [2] on the artificially generated ECG signal and the corresponding signal derived (“s”) interval measurements series  $RR(n)$  and  $QT(n)$  were denoted as datasets  $A_s$ ,  $B_s$  and  $C_s$  for each case of possible dependency.

Additionally, artificial ECG signals were contaminated with pre-recorded noise from the MIT-BIH Noise Stress Test Database [7] corresponding to baseline wandering, muscular artefacts and electrode movement artefacts. The first noise leads in the database were resampled to 500 Hz and multiplied by a constant factor to get a predefined SNR when added to the artificial ECG. The contaminated artificial ECG signals were also processed following [2]. Potential RR outliers were rejected and  $RR(n)$  and  $QT(n)$  series of 350 consecutive beats were taken as new noise driven (“v”) test data (datasets  $A_v$ ,  $B_v$  and  $C_v$ ). The true spectra of the simulated series can be obtained directly from  $\lambda_{QT}^2$  and the simulation coefficients. The true reference power variability measures  $\tilde{P}_E^B$  were calculated for both models (RR simulated from REST and TILT) and used as references for all  $QT(n)$  series from all datasets derived from the model. The percentage error  $\varepsilon$  of the ARARX model in quantification of the QTV fraction correlated with HRV is the difference between the ratio calculated in equation (6) and the reference value:

$$\varepsilon = \left( R_{QT/W_{RR}}^B - \frac{\tilde{P}_{QT/W_{RR}}^B}{\tilde{P}_{QT/W_{RR}}^B + \tilde{P}_{QT/W_{QT}}^B} \right) \times 100. \quad (7)$$

### 3. Results and discussion

The methods described were implemented using MATLAB System Identification Toolbox. The measures were estimated considering frequency bands ( $B$ ) typically used in HRV studies: low frequency ( $B=LF$ ) as 0.04-0.15 Hz and high frequency ( $B=HF$ ) as 0.15-0.4Hz. Total power ( $B=TP$ ) was taken from 0.04 Hz to the highest frequency present in each spectrum.

#### 3.1. Automatic delineation effect

The results from series measured on the artificial ECG signal (datasets  $A_s$ ,  $B_s$  and  $C_s$ ) presented errors slightly higher than in raw clean simulated series ( $A_c$ ,  $B_c$  and  $C_c$ ). The distribution of the errors ( $\varepsilon$ ) in the quantification of the

QTV fraction correlated with HRV can be found in Fig. 3, for each frequency band. In  $A_c$ ,  $B_c$  and  $C_c$ ,  $\varepsilon \leq 5\%$  for about 77% of the series in TP band, 72% in LF and 80% in HF, while in  $A_s$ ,  $B_s$  and  $C_s$   $\varepsilon \leq 5\%$  for about 72% of the series in TP band, 66% in LF and 73% in HF. The mean ( $\bar{\varepsilon}$ ) and standard deviation ( $\sigma_\varepsilon$ ) of  $\varepsilon$  found in each dataset and frequency band are presented in Table 1:  $\bar{\varepsilon} \leq 4.5\%$  ( $\sigma_\varepsilon \leq 15\%$ ) for  $A_c$ ,  $B_c$  and  $C_c$  while  $\bar{\varepsilon} \leq 5.5\%$  ( $\sigma_\varepsilon \leq 16\%$ ) for  $A_s$ ,  $B_s$  and  $C_s$ , representing a small and non relevant performance decrease.

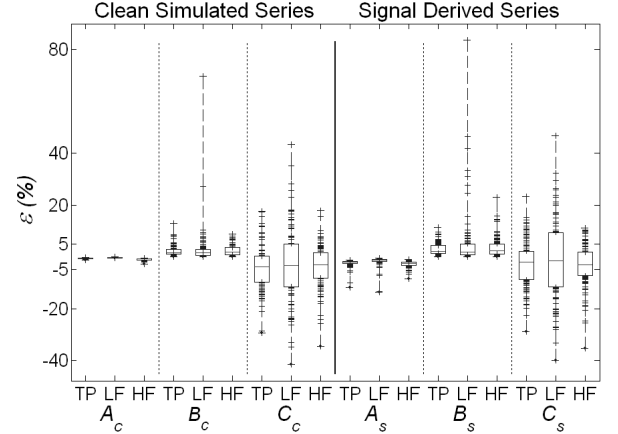


Figure 3. Box-and-whisker plot of  $\varepsilon$  by frequency band in  $A_c$ ,  $B_c$ ,  $C_c$ ,  $A_s$ ,  $B_s$  and  $C_s$  (+ for  $\varepsilon$  out of quartiles box).

#### 3.2. Noise contamination

We found adequate segments and valid models for over 99% of the series for  $\text{SNR} \geq 20\text{dB}$ . Lower SNR reduced the number of segments to near 85% of the situations with 15dB and less than 20% with 10dB. As expected, the quality of the estimation decreased with SNR level. Dataset  $A_v$  is the most affected with  $\bar{\varepsilon}$  reaching 10% in TP and 14% in HF for SNR of 30 dB. For dataset  $B_v$ ,  $\bar{\varepsilon} \leq 5.5\%$  ( $\sigma_\varepsilon \leq 8\%$ ) for all frequency bands and  $\text{SNR} \geq 10\text{ dB}$ . In dataset C,  $\bar{\varepsilon} \leq 4\%$  ( $\sigma_\varepsilon \leq 20\%$ ) in LF and  $\bar{\varepsilon} \leq 9\%$  ( $\sigma_\varepsilon \leq 8\%$ ) in TP,  $\text{SNR} \geq 20\text{ dB}$ ; HF is more affected with  $\bar{\varepsilon} \leq 14.5\%$  ( $\sigma_\varepsilon \leq 10.5\%$ ). Looking to the distribution of the estimated variability measures  $P_{QT/W_{RR}}^B$  (Fig. 4), considering all noise types for datasets  $C_c$ ,  $C_s$  and  $C_v$  (SNR from 30dB to 15dB) the estimated values kept near the reference even for SNR of 15 dB. No relevant differences were found between noise types nor REST and TILT situations. Equivalent results were found for all datasets, with the lowest errors in dataset B for all SNR levels. In spite of A and C situations presented the same level of error in the power estimation, as one of the fractions does not exist in dataset A, QTV power is lower, what justifies higher errors in fraction quantification (%).

Table 1. Mean and standard deviation of  $\varepsilon$  in datasets  $A_c$ ,  $B_c$ ,  $C_c$ ,  $A_s$ ,  $B_s$  and  $C_s$ . (% ,  $mean \pm sd$ )

	series $A_c$	series $B_c$	series $C_c$	series $A_s$	series $B_s$	series $C_s$
$B = TP$	$-0.67 \pm 0.20$	$2.21 \pm 2.02$	$4.16 \pm 8.89$	$-2.39 \pm 1.45$	$3.01 \pm 2.44$	$-2.70 \pm 9.21$
$B = LF$	$-0.29 \pm 0.11$	$3.09 \pm 7.53$	$-3.05 \pm 14.81$	$-1.80 \pm 1.99$	$5.47 \pm 11.42$	$0.87 \pm 15.61$
$B = HF$	$-0.94 \pm 0.40$	$2.33 \pm 2.06$	$-3.76 \pm 8.33$	$-2.84 \pm 1.18$	$3.62 \pm 3.94$	$-3.43 \pm 8.13$

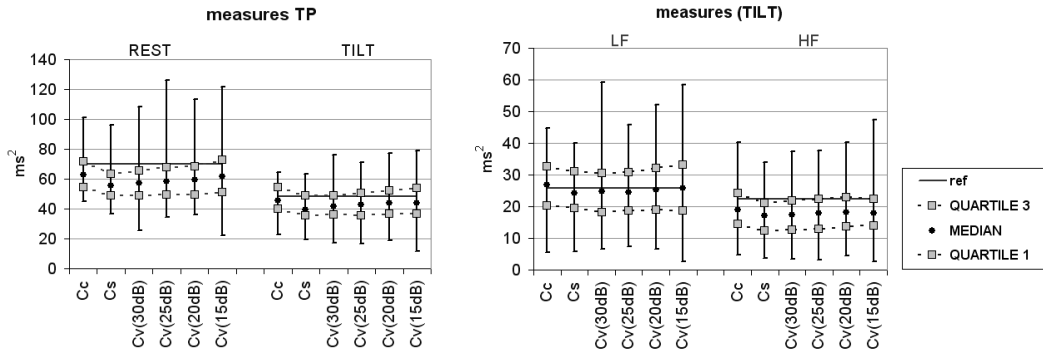


Figure 4. Distribution of  $P_{QT/W_{RR}}^B$  for datasets  $C_c$ ,  $C_s$  and  $C_v$ . Reference measures from the simulation model.

## 4. Conclusions

Exploring short term RR and QT interaction in clinical routine data and facing noise contamination is a challenging and complex problem. This study evaluated the robustness of a methodology to assess this relation by automatic delineation and linear low order parametric modelling. The results pointed out that no relevant performance decrease results from delineation. The quality decrease in estimation due to ECG noise does not degrade the variability measures to nonusefull levels with moderate contamination levels. Noisier ECG records will require an improvement of the delineation system.

The results indicated that the joint performance of the two systems (delineation plus variability analysis) is satisfactory for SNR levels over 20 dB, namely in the more realistic clinical case of a mixture of QT dependencies. Clinical interpretation studies about the value of the uncorrelated fraction can now be faced within the framework of this modelling.

## Acknowledgements

This work was supported by the projects TIC2001-2167-C02-02 from MCYT/FEDER, P075/2001 from CONSID-DGA (Spain) and the integrated action HP2001-0031/CRUP-E26/02. R Almeida would like to thank the grant SFRH/BD/5484/ 2001 supported by FCT and ESF.

## References

- [1] Almeida R, Pueyo E, Martínez JP, Rocha AP, Olmos S, Laguna P. A parametric model approach for quantification of short term QT variability uncorrelated with heart rate variability. In Computers in Cardiology 2003. Thessaloniki: IEEE, 2003; 165–168.
- [2] Martínez JP, Almeida R, Olmos S, Rocha AP, Laguna P. Wavelet-based ECG delineator: evaluation on standard databases. IEEE Trans Biomed Eng 2004;51:570–581.
- [3] Porta A, Baselli G, Caiani E, Malliani A, Lombardi F, Cerutti S. Quantifying electrocardiogram RT-RR variability interactions. IEEE Trans Biomed Eng 1998;36:27–34.
- [4] Ljung L. System identification theory for the user. Second edition. Prentice Hall PTR, 1999.
- [5] Mateo J, Laguna P. Improved heart rate variability signal analysis from the beat occurrence times according to the ipfm model heart timing signal. IEEE Trans Biomed Eng 2000; 47:985–996.
- [6] Marple SL. Digital spectral analysis with applications. Prentice Hall, 1987.
- [7] Moody GB, Mark RG. The MIT-BIH arrhythmia database on CD-ROM and software for use with it. In Computers in Cardiology 1990. IEEE Computer Society Press, 1990; 185–188.

Address for correspondence:

Rute Almeida  
 Departamento de Matemática Aplicada  
 Faculdade de Ciências da Universidade do Porto  
 Rua do Campo Alegre, 687; 4169-007, Porto, Portugal.  
 E-mail address: rbalmeid@fc.up.pt.